Josephson junction dynamics in the presence of 2π - And 4π -periodic supercurrents

Domínguez, F.; Kashuba, O; Bocquillon, E; Wiedenmann, J; Deacon, R. S.; Klapwijk, T. M.; Platero, G; Molenkamp, Laurens W.; Trauzettel, B.; Hankiewicz, E. M.

DOI
10.1103/PhysRevB.95.195430

Publication date
2017

Document Version
Final published version

Published in
Physical Review B (Condensed Matter and Materials Physics)

Josephson junction dynamics in the presence of 2π- and 4π-periodic supercurrents

F. Domínguez,[1] O. Kashuba,[1] E. Bocquillon,[2,3] J. Wiedenmann,[2] R. S. Deacon,[4,5] T. M. Klapwijk,[6] G. Platero,[7] L. W. Molenkamp,[2] B. Trauzettel,[1] and E. M. Hankiewicz[1]

[1]*Institut für Theoretische Physik und Astrophysik, Universität Würzburg, D-97074 Würzburg, Germany*

[2]*Physikalisches Institut (EP3), Universität Würzburg, D-97074 Würzburg, Germany*

[3]*Laboratoire Pierre Aigrain, Ecole Normale Supérieure-PSL Research University, CNRS, Université Pierre et Marie Curie-Sorbonne Universités, Université Paris Diderot-Sorbonne Paris Cité, 24 rue Lhomond, 75231 Paris Cedex 05, France*

[4]*Advanced Device Laboratory, RIKEN, 2-1 Hirosawa, Wako-shi, Saitama, 351-0198, Japan*

[5]*Center for Emergent Matter Science, RIKEN, 2-1 Hirosawa, Wako-shi, Saitama, 351-0198, Japan*

[6]*Kavli Institute of Nanoscience, Faculty of Applied Sciences, Delft University of Technology, Lorentzweg 1, 2628 CJ Delft, The Netherlands*

[7]*Instituto de Ciencia de Materiales, CSIC, Cantoblanco, E-28049 Madrid, Spain*

(Received 25 January 2017; published 30 May 2017)

We investigate theoretically the dynamics of a Josephson junction in the framework of the resistively shunted junction model. We consider a junction that hosts two supercurrent contributions: a 2π and a 4π periodic in phase, with intensities $I_{2\pi}$ and $I_{4\pi}$, respectively. We study the size of the Shapiro steps as a function of the ratio of the intensity of the mentioned contributions, i.e., $I_{4\pi}/I_{2\pi}$. We provide detailed explanations where to expect clear signatures of the presence of the 4π-periodic contribution as a function of the external parameters: the intensity ac bias $I_{\rm ac}$ and frequency $\omega_{\rm ac}$. On the one hand, in the low ac-intensity regime (where $I_{\rm ac}$ is much smaller than the critical current $I_{\rm c}$), we find that the nonlinear dynamics of the junction allows the observation of only even Shapiro steps even in the unfavorable situation where $I_{4\pi}/I_{2\pi} \ll 1$. On the other hand, in the opposite limit ($I_{\rm ac} \gg I_{\rm c}$), even and odd Shapiro steps are present. Nevertheless, even in this regime, we find signatures of the 4π supercurrent in the beating pattern of the even step sizes as a function of $I_{\rm ac}$.

DOI: 10.1103/PhysRevB.95.195430

I. INTRODUCTION

A topological superconductor forms a new state of quantum matter and possesses a pairing gap in the bulk and gapless surface states which in some cases form nontrivial Majorana bound states [1–3]. The Majorana bound states can be interpreted as fermionic particles equivalent to their own antiparticles, and have potential applications in fault-tolerant topological quantum computation [4–7]. Additionally to p-wave superconductors like Sr_2RuO_4 or $d+id$ superconductors on hexagonal lattices [8,9], new platforms to host Majorana bound states based on proximitizing ordinary singlet-spin superconductor to a material with a strong spin-orbit interaction were proposed [10–13]. In addition to spectroscopic signatures of the Majorana bound states [14–16], recent experiments on Josephson junctions (JJs) based on Rashba wires or topological insulators, which could show topologically nontrivial modes, have attracted a lot of attention [17–20].

Josephson junctions containing a topologically protected Andreev level exhibit 4π periodicity in respect to the superconducting phase difference φ [10–13,21–23]. Hence, the measurement of topological properties of the JJ involves a probing of the periodicity of the electronic properties of the junction. This can be achieved by means of the ac Josephson effect [10]. For example, when the JJ is biased by dc and ac currents $I_0 + I_{\rm ac}\sin(\omega_{\rm ac}t)$, the average voltage develops plateaus at integer multiples of $\hbar\omega_{\rm ac}/2e$, i.e., $V = n\hbar\omega_{\rm ac}/2e$, n being an integer number [24]. These plateaus are known as Shapiro steps and are the result of a synchronization process between the external driving frequency $\omega_{\rm ac}$ and the frequency of the junction ω_0. Their experimental measurement allows to establish a direct correspondence between the periodicity of the electronic properties of the junction and an observable because when the supercurrent is 4π periodic, only even multiples of $\hbar\omega_{\rm ac}/2e$ (even Shapiro steps) appear. The accuracy and universality of this relation has made the Shapiro steps the basis of the international voltage standard with an accuracy of one part per billion. Alternatively, one can measure the voltage emission spectrum [20]. In this case, the 4π periodicity manifests itself as a resonance line separated by the fractional frequency $\omega_0/2$ of the junction. Nevertheless, these proposals need to be performed carefully, due to several side effects. For example, relaxation processes may break parity conservation yielding a 2π-periodic supercurrent [10,25,26]. Furthermore, finite-size effects, and the coexistence of the 4π-periodic Andreev state together with ordinary Andreev levels with a 2π periodicity, could obscure completely the measurement of the 4π-periodic signal. Proposals based on dynamical transitions allow to overcome these difficulties [27–36]. Further proposals overcome some of these problems by studying the skewness of the 4π-periodic supercurrent profile [37,38] or the phase-dependent thermal conductance with minimum at $\varphi = \pi$ independent of the barrier strength in the heat transport setup [39].

During the last years, some experiments were performed in JJs where the presence of the 4π-periodic Andreev level may be responsible for the observations. In Refs. [17–19], even Shapiro steps stand alone at low values of the applied external ac frequency $\omega_{\rm ac}$ and ac intensity $I_{\rm ac}$. Then, increasing $\omega_{\rm ac}$ and/or $I_{\rm ac}$, odd Shapiro steps also appear. A similar phenomenon was observed in Ref. [20], where the voltage emission spectrum was measured as a function of an external dc current bias I_0. For low I_0, a signal with the fractional frequency $\omega_0/2$ appears, while for increasing I_0, one observes a clear transition towards the integer frequency ω_0. The overall

response will be studied on a phenomenological level by the resistively shunted junction (RSJ) model [20,31] carrying two superconducting contributions $I_{2\pi}\sin(\varphi)$ and $I_{4\pi}\sin(\varphi/2)$. From now on, we will call it 2 supercurrents RSJ (2S-RSJ) model. We will explain the regime of parameters that gives rise to the $4\pi \to 2\pi$ transition which can be seen in experiments.

Furthermore, we explain how to extend our analysis of the 2S-RSJ model to the presence of an additional 8π-periodic supercurrent. Such a contribution can originate from parafermions in interacting topological junctions [40–42]. Similar to the 4π case, it is very difficult to measure directly the 8π periodicity. In turn, we believe that it could be possible to see the effects of the 8π-periodic term in the Shapiro experiment or by measuring the voltage emission spectrum.

The outline of the paper is as follows. In Sec. II, we present the 2S-RSJ model, with 2π- and 4π-periodic dependence on the phase. Then, in Sec. III, we provide a qualitative explanation of the 2S-RSJ model dynamics by introducing the modified washboard potential (WP). In particular, the time-dependent WP allows for a very intuitive understanding of the Shapiro step formation as well as reasons for the discrimination between the odd and the even steps. We summarize our knowledge on the nonstationary topological Josephson effect in form of a "phase diagram." Finally, in Sec. IV, we consider two limits of the 2S-RSJ model, the low $I_{ac} \ll I_c$ and the high $I_{ac} \gg I_c$ intensity limits, where I_c is the critical current of the JJ. We solve the 2S-RSJ model analytically in these limits of interest. In the low-intensity limit ($I_{ac} \ll I_c$), we establish the relation between the emission spectrum experiment and the Shapiro experiment in terms of the dc voltage. In addition, we study the step width as a function of ω_{ac}. In the high-intensity limit ($I_{ac} \gg I_c$), we explain the beating pattern appearing in the even Shapiro step widths as a function of I_{ac}.

II. 2S-RSJ MODEL

The RSJ model was introduced in Refs. [43–45]. Under this approach, the JJ dynamics is reduced to the study of an equation of motion, which can be interpreted as a parallel circuit, including three arms: the Josephson junction, a resistive and a capacitive arm. Here, we will restrict ourselves to the study of the overdamped limit of the 2S-RSJ model, neglecting the capacitive arm [see Fig. 1(a)] [31,33]. This simple model contains the basic ingredients to describe the phase dynamics phenomenologically. The equation of motion describing the circuit is given by

$$I_{ext}(t) = \frac{\hbar}{2eR}\frac{d\varphi}{dt} + I(\varphi), \tag{1}$$

with $I(\varphi) = I_{2\pi}\sin(\varphi) + I_{4\pi}\sin(\varphi/2)$ and $I_{ext}(t) = I_0 + I_{ac}\sin(\omega_{ac}t)$. As we explained above, the 4π-periodic term $I_{4\pi}\sin(\varphi/2)$ is of special interest because it may originate from the presence of topological superconductivity. Writing Eq. (1) we made several assumptions: the supercurrent coefficients $I_{2\pi}$ and $I_{4\pi}$ and the resistance R are constant, independently of the applied bias $I_{ext}(t)$. This assumption sets a restriction on the energy gap between adjacent Andreev levels, and from Andreev levels to the continuum, and the applied current bias $I_{ext}(t)$, since nonadiabatic transitions may take place. Besides, the 2S-RSJ model neglects also other dynamical

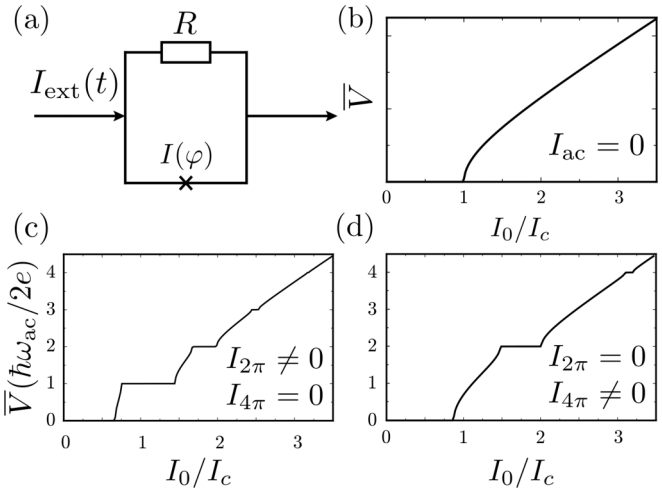

FIG. 1. (a) Scheme of the RSJ circuit. (b) $\overline{V}$ as a function of I_0, with $I_{ac} = 0$. The voltage becomes finite for $I_0 \geqslant I_c$. The dependency is $\overline{V} \sim R\sqrt{I_0^2 - I_c^2}$. (c), (d) We represent the voltage as a function of I_0, with $I_{ac} \neq 0$, and $I_{4\pi} = 0$ (c), and $I_{2\pi} = 0$ (d). Thus, the periodicity of the supercurrent is reflected in the parity of the Shapiro steps. In panel (c) [(d)], we show Shapiro steps at integer (even) multiples of $\hbar\omega_{ac}/2e$.

processes such as quasiparticle poisoning [25,26] or dynamical transitions that might change the phase periodicity and, thus, the intensities $I_{2\pi}$ and $I_{4\pi}$ [27,29,31–33]. It is possible to omit these effects when the quasiparticle poisoning time $t_{qp} \sim \mu$s [46] is much larger than the largest time scale of the biased junction, i.e., $\mathrm{Max}(\tau_R^k, 1/\omega_{ac})$ [32]. Here, $\tau_R^k = 1/(eRI_k)$, with $I_k = I_c|J_k(2eRI_{ac}/\hbar\omega_{ac})|$, is the transient time during which the phase becomes periodic in time, after a quasiparticle poisoning event is produced. Note that we have used the kth-Bessel function $J_k(x)$. Furthermore, we expressed the functionality of the supercurrent simply as a sum of two sinusoidal contributions, which differs from a microscopic derivation.

The solution of this differential equation provides the induced voltage $V(t) = \hbar\dot{\varphi}(t)/2e$, where $\dot{\varphi}(t)$ is a periodic function with period $T_{4\pi}$, and frequency $\omega_0 = 4\pi/T_{4\pi}$. Furthermore, the average voltage and the frequency are proportional to each other by means of $\omega_0 = 2e\overline{V}/\hbar$, where the overline denotes the average over time.

The general features of the current-voltage dispersion can be summarized as follows: Starting from the dc bias, i.e., $I_{ac} = 0$, we observe that in order to generate a voltage, the current bias I_0 must exceed the critical value $I_c \equiv \max\{I(\varphi)\}$ [see Fig. 1(b)]. In this situation, part of the driving current goes through the dissipative arm of the circuit and therefore a voltage is generated. The average voltage can be obtained analytically either for $I_{2\pi} = 0$ or $I_{4\pi} = 0$, and is given by $\overline{V} = R\sqrt{I_0^2 - I_c^2}$. In the presence of an ac current, the voltage develops Shapiro steps at integer multiples of $\hbar\omega_{ac}/2e$. In Figs. 1(c) and 1(d) we show an example of the Shapiro experiment only considering $I_{2\pi}$ and $I_{4\pi}$, respectively. We can see that in the case of a pure 4π- (2π-) periodic supercurrent, the voltage contains only even (all) multiples of $\hbar\omega_{ac}/2e$.

When both contributions $I_{2\pi}$ and $I_{4\pi}$ are present the nonlinear dynamics of the junction governs the low-bias

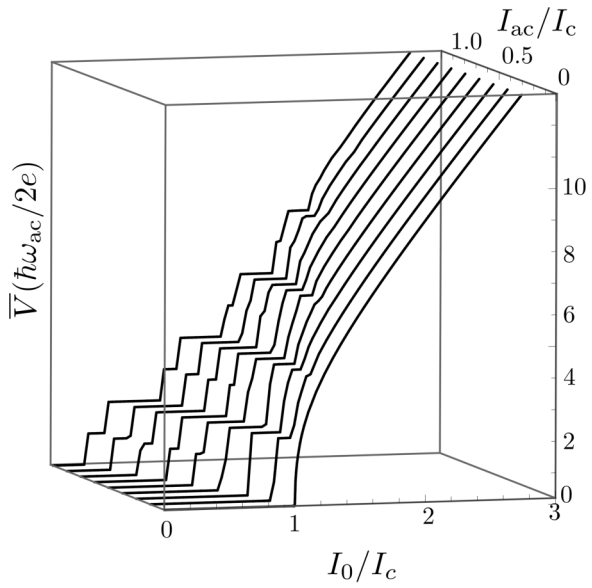

FIG. 2. I-$\overline{V}$ curves for different values of $I_{ac} = 0$ up to I_c, with $I_{4\pi}/I_{2\pi} = 0.5$, $\omega_{ac} = 0.2(2eRI_c/\hbar)$. We observe the appearance of odd steps, when $I_{ac} \gtrsim I_{4\pi}$.

regime and gives rise to a very interesting situation: it is possible to find only even Shapiro steps for a finite range of I_{ac} and even for $I_{4\pi} \ll I_{2\pi}$ [31]. This phenomenon has been observed experimentally [17–19], and as we will explain below, we can relate it to the power spectrum of the voltage [20]. As an example of this, we show in Fig. 2 I-$\overline{V}$ curves for $I_{ac} = 0$ up to $I_{ac} = I_c$, and $I_{4\pi}/I_{2\pi} = 0.5$. For low values of I_{ac} we find only even steps, while increasing $I_{ac} \gtrsim I_{4\pi}$, the odd steps emerge. In the following sections, we will present detailed qualitative and quantitative explanations about the parameter regime where to expect only even Shapiro steps.

III. WASHBOARD POTENTIAL

We can picture the phase dynamics of the 2S-RSJ model as a massless particle sliding on top of a potential, adapting its velocity instantaneously to its slope. In order to see this, we rewrite Eq. (1) as $(\hbar/2eR)\dot{\varphi} = -\partial U(\varphi,t)/\partial\varphi$, where

$$U(\varphi,t) = -I_{ext}(t)\varphi + \int d\varphi\, I(\varphi) \tag{2}$$

is the, so-called, washboard potential. Here, the external drive term $I_{ext}(t)\varphi$ controls the slope, and on top of that, the supercurrent contribution modulates the WP profile sinusoidally [see Fig. 3(a)]. We study the static and dynamical WP, where $I_{ac} = 0$ and $I_{ac} \neq 0$, respectively.

A. Static WP

In the absence of ac bias, the I-V curves exhibit a zero voltage drop for $I_0 \leqslant I_c$. This fact is reflected in the WP as minima where the particle rests [see Fig. 3(a)]. Increasing I_0 above the critical value I_c, the local minima in the tilted potential vanish, and then, the particle slides along the WP passing intervals of flatter and steeper slopes. In this situation, the motion of the particle alternates between slow and rapid

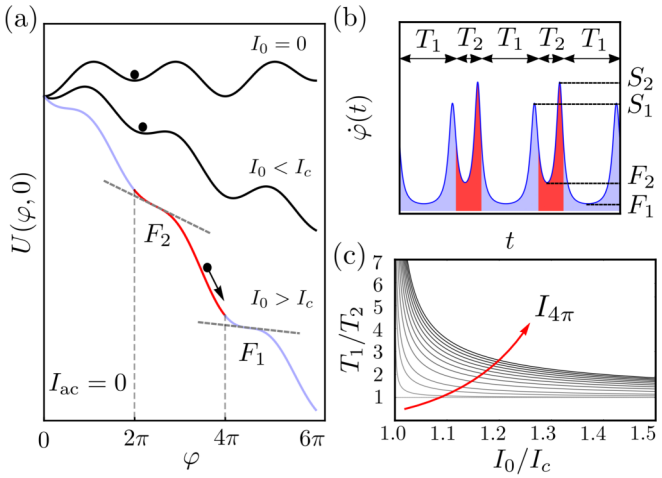

FIG. 3. (a) The washboard potential with $I_{ac} = 0$ as a function of φ for three different values of I_0: top curve $I_0 = 0$, $I_0 < I_c$ middle curve, and $I_0 > I_c$ bottom curve. The dashed lines remark the slope of the WP at the odd (F_1) and even (F_2) flattest regions. We highlight the even and odd sectors in red and blue, respectively. (b) We show the time evolution of $\dot{\varphi}(\tau)$ [31]. We mark in blue (red) the odd (even) sectors according to Eqs. (3) and (4). Besides, we can extract from the WP the maxima of $\dot{\varphi}(t)$: $S_1 \approx I_0 + I_c - \sqrt{2}I_{4\pi}$, $S_2 = I_0 + I_c$, $F_1 = I_0 - I_c$, and $F_2 \approx I_0 - I_c + \sqrt{2}I_{4\pi}$, being the steepest and the flattest slopes in each sector, and the equation $(\hbar/2eR)\dot{\varphi} = -\partial U(\varphi,t)/\partial\varphi$ relates the slope and the velocity at each time. (c) We represent the ratio T_1/T_2 as a function of I_0 for different values of $I_{4\pi}/I_{2\pi}$ from zero to one.

sectors. We can see the WP profile in Fig. 3(a), and the resulting time evolution of $\dot{\varphi}(t)$ in Fig. 3(b), characterized by narrow peaks and flat regions.

The presence of the 4π-periodic contribution modifies the WP introducing a relative phase between the sectors $\varphi_{odd} = [4(l-1)\pi, 4(l-1/2)\pi]$ and $\varphi_{even} = [4(l-1/2)\pi, 4l\pi]$, l being an integer number. From now on, φ_{odd} and φ_{even} will be called odd and even sectors, respectively. In the odd sectors, the 4π term contributes with opposite phase to I_0 yielding a flatter slope on the WP. On the other hand, the 4π current adds to the dc current I_0 in the even sectors, and therefore the slope of the flatter regions becomes more negative, whereas in the odd sectors the 4π term is subtracted from I_0. We can observe the slope difference between both sectors in Fig. 3(a), where the odd (even) sectors are highlighted in blue (red) [36]. The resulting $\dot{\varphi}(t)$ changes accordingly, and shows different maxima depending on the sector parity: the odd sectors show the steepest and flattest slopes $S_1 \approx I_0 + I_c - \sqrt{2}I_{4\pi}$ and $F_1 = I_0 - I_c$, respectively, while the even sectors $S_2 = I_0 + I_c$ and $F_2 \approx I_0 - I_c + \sqrt{2}I_{4\pi}$ [see Fig. 3(b)]. Note that S_1 and F_2 are approximate for $I_{4\pi}/I_{2\pi} \ll 1$.

The observed changes of slope cause differences between the time spent in each sector, which is given by

$$T_1 = \frac{\hbar}{2eR}\int_0^{2\pi} \frac{d\varphi}{I_0 - I_{2\pi}\sin(\varphi) - I_{4\pi}\sin(\varphi/2)}, \tag{3}$$

$$T_2 = \frac{\hbar}{2eR}\int_{2\pi}^{4\pi} \frac{d\varphi}{I_0 - I_{2\pi}\sin(\varphi) - I_{4\pi}\sin(\varphi/2)}, \tag{4}$$

where T_1 (T_2) is the time spent by the particle in the odd (even) sector. Equations (3) and (4) differ on the integration range, which introduces a relative sign in $\sin(\varphi/2)$. In the odd (even) sector $\sin(\varphi/2)$ is always positive (negative), contributing to a decrease (increase) of the denominator. Thus, by construction $T_1 \geqslant T_2$. This is in accordance to the observed differences between F_1 and F_2. Therefore, the ratio T_1/T_2 indicates the impact of the 4π-supercurrent contribution on the phase dynamics. For $T_1/T_2 \gg 1$ ($T_1/T_2 \sim 1$), the particle spends most of the time in the odd (both) sectors yielding an effective 4π (2π) WP profile. In Fig. 3(c), we plot the ratio T_1/T_2 as a function of I_0, for different values of $I_{4\pi}$. We observe that for $I_0 \sim I_c$, the ratio $T_1/T_2 \gg 1$. Then, increasing I_0 causes a rapid decay of the ratio T_1/T_2 towards 1. Remarkably, we can observe a range of I_0 where $T_1/T_2 \gg 1$, even for very small ratios $I_{4\pi}/I_{2\pi} \sim 0.05$. This means that the junction exhibits a 4π-periodic dynamics for a finite range of I_0. Naturally, the smaller the ratio $I_{4\pi}/I_{2\pi}$ is, the smaller the range of I_0 becomes. This nonadditive phenomenon reveals the highly nonlinear dynamics of the 2S-RSJ model.

We can roughly estimate T_1 and T_2 considering that the particle spends most of the time in the flattest regions and, thus, $T_1 \propto 1/F_1 = 1/(I_0 - I_c)$ and $T_2 \propto 1/F_2 \approx 1/(I_0 - I_c + \sqrt{2}I_{4\pi})$. Note that in the limit of $I_0 \gtrsim I_c$, T_1 becomes much larger than T_2. In turn, $I_0 - I_c \gg I_{4\pi}$ leads to $T_1 \sim T_2$. These considerations on a dc-driven junction explain experimental results on the anomalous emission at $\omega_0/2$ of topological Josephson junctions [20], as will be detailed later.

B. Dynamical WP

We now introduce the effects of the ac-current bias $I_{ac}\sin(\omega_{ac}t)$, assuming the adiabatic approximation, i.e., $\hbar\omega_{ac}/2eRI_c \ll 1$ [36]. It enhances or reduces the effect of I_0 depending on their relative sign. At the time periods when $I_0 + I_{ac}\sin(\omega_{ac}t) < I_c$, the current bias recovers the minima, where the particle stops. In order to represent together in a single plot the dynamical WP at different times, we show in Fig. 4 a renormalized WP given by $\tilde{U}(\varphi,t) = [I_0/|I_{ext}(t)|]U(\varphi,t)$, so that U and $\tilde{U}$ coincide for $I_{ac} = 0$. Thus, we separate visually the average tilting from the ac-bias slope, while we keep the local sign of the slope unchanged at any time. The regions with positive slope (marked red) are impenetrable for the particle at the given moment of time. The periodic appearance of the red intervals realizes a turnstile mechanism, which allows the phase to propagate an integer multiple m of green intervals between the minima per cycle. This manifests itself in the relation $\omega_0 = n\omega_{ac}$, where the particle slides through m green intervals of total length $2\pi n$ until it stops. Shapiro step arises if the resonance (with fixed n and m) holds for a finite range of I_0. This means that the different tilting I_0 of the WP is compensated by the stopping periods. Thus, the particle's average speed ($\langle\dot{\varphi}\rangle$) remains constant.

Interestingly, we can find a situation where only the 4π contribution becomes visible. When the ac current is set such that it fulfills $|F_2| \gtrsim I_{ac}\sin(\omega_{ac}t) \gtrsim |F_1|$, the WP recovers temporarily the minima in the odd sectors only, being separated by a phase difference of 4π and not 2π (see bottom curve in Fig. 4). Thus, the periodicity of the junction is effectively that of a pure 4π-periodic one. Hence, we expect to observe only even Shapiro steps since $2\pi n = 4\pi m$. On the other hand, for the period of time where $|F_2| \lesssim I_{ac}\sin(\omega_{ac}t)$, the particle is temporarily stopped at each sector, yielding any multiple of Shapiro step (see top curve in Fig. 4).

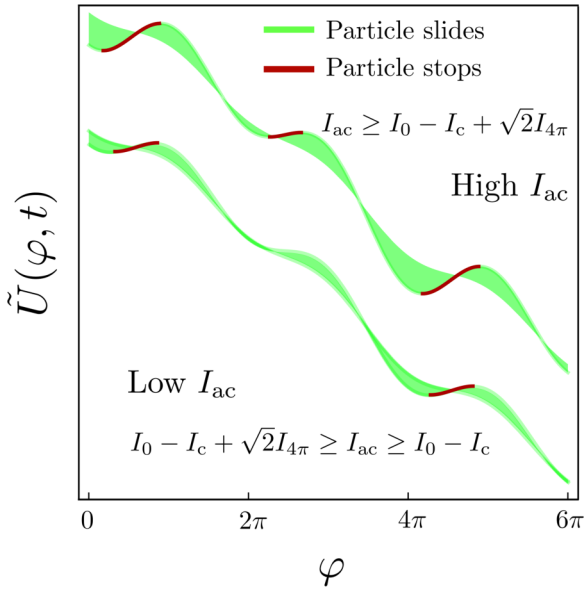

FIG. 4. The renormalized washboard potential $\tilde{U}(\varphi,t)$ as a function of φ for two different values of the external bias $I_0 - I_c < I_{ac} < I_0 - I_c + \sqrt{2}I_{4\pi}$ (bottom curve) and $I_0 - I_c + \sqrt{2}I_{4\pi} < I_{ac}$ (top curve). We highlight in green the sectors where $\partial\tilde{U}/\partial\varphi < 0$ and in red $\partial\tilde{U}/\partial\varphi > 0$.

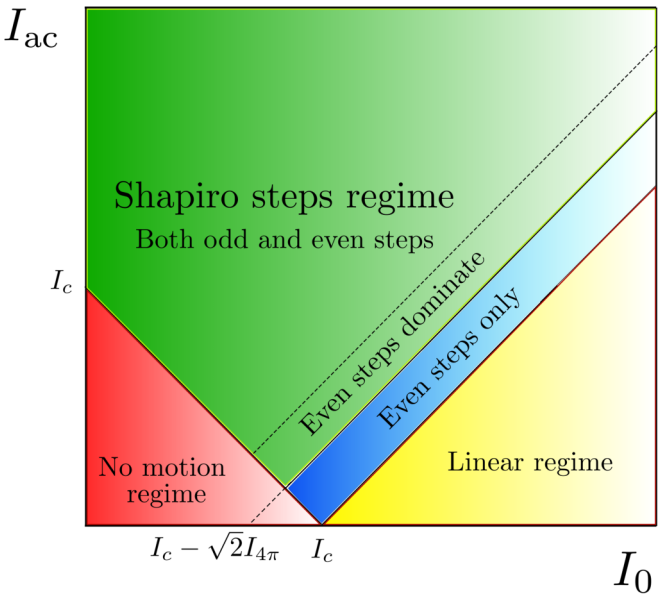

FIG. 5. Phase diagram of the voltage as a function of I_0 and I_{ac}. We differentiate between "no motion regime" (red area), where $\overline{V} = 0$. The "linear regime" (yellow area), where there is no Shapiro steps but $\overline{V} \neq 0$. Finally, the "Shapiro steps regime" (green and blue areas). Remarkably, following the WP considerations we expect to observe only even steps in the blue area, i.e., for $I_0 - I_c + \sqrt{2}I_{4\pi} \gtrsim I_{ac} \gtrsim I_0 - I_c$.

We summarize these qualitative results in Fig. 5, where we estimate the parameter regime of the Shapiro steps as a function of I_{ac} and I_0. We differentiate between three regimes: "no motion regime" (red area), limited by $I_0 + I_{ac} < I_c$. Here, the WP exhibits always minima where the particle rests, yielding a zero average voltage $\overline{V} = 0$. The "linear regime" (yellow area) extends over $I_0 - I_c > I_{ac}$, where the WP cannot stop the particle at any time, yielding a finite voltage without developing steps. Finally, the "Shapiro steps regime" (green and blue areas) is the region limited by $I_0 - I_c < I_{ac}$ and $I_0 + I_{ac} > I_c$. Following the arguments presented above, we distinguish an inner blue region $I_0 - I_c + \sqrt{2}I_{4\pi} \gtrsim I_{ac} \gtrsim I_0 - I_c$ where we expect to observe the even steps only. Increasing further I_{ac}, we expect to observe a crossover where odd steps appear together with even steps, with a dominating even steps contribution. Then, for $I_{ac} > I_0 - I_c + \sqrt{2}I_{4\pi}$ we expect to have even and odd Shapiro steps, without any clear dominance.

Higher Shapiro steps are placed at larger values of I_0. Therefore, following the previous reasoning, in order to generate the higher steps, we need to make the relation $I_0 - I_c - I_{ac}$ negative. Considering a constant I_c, this can be achieved by increasing further I_{ac}, as it is shown in Fig. 2. Thus, we will find only even steps if in addition the ac intensity fulfills $I_{ac} \leqslant I_0 - I_c + \sqrt{2}I_{4\pi}$.

We now understand the underlying reason for the observation of even Shapiro steps in terms of the WP. Note, however, that in all our arguments presented so far, we have assumed an adiabatic evolution of the WP, i.e., $\hbar\omega_{ac}/2eRI_c \ll 1$. In order to better understand the role played by ω_{ac}, we perform a perturbative approach to the equation of motion in the next section. We show below that the effect of increasing the value of ω_{ac} has a similar effect as increasing I_0 [31]. This can be understood in the following way: since the Shapiro steps occur at $\omega_0 = n\omega_{ac}$, where $n \in \mathbb{N}$, in order to fulfill $\omega_0 = n\omega_{ac}$, we will need to increase ω_0 by increasing I_0. Nevertheless, this reasoning is vague and deserves a quantitative study.

C. Extension of the 2S-RSJ model: Searching for parafermions

In the presence of an additional 8π-periodic supercurrent $I_{8\pi}\sin(\varphi/4)$, the WP acquires four different flattest and steepest slopes, i.e., F_1, F_2, F_3, F_4 and S_1, S_2, S_3, S_4, respectively. These slopes correspond to the sectors $\varphi_1 = [8(l-1)\pi, 8(l-1/4)\pi]$, $\varphi_2 = [8(l-1/4)\pi, 8(l-1/2)\pi]$, $\varphi_3 = [8(l-1/2)\pi, 8(l-3/4)\pi]$, and $\varphi_4 = [8(l-3/4)\pi, 8l\pi]$, l being an integer number. Assuming that $I_{2\pi} \geqslant I_{4\pi} \geqslant I_{8\pi}$, we find that $F_1 > F_3 > F_2 > F_4$, which is naturally related to the way the superconducting phases $\sin(\varphi)$, $\sin(\varphi/2)$, $\sin(\varphi/4)$ add up. Following an analogous reasoning as previously, we find a window of I_{ac}, in which only Shapiro steps that are multiples of 4 arise. This window occurs for $I_0 - I_c + \frac{4}{5}I_{8\pi} \geqslant I_{ac} \geqslant I_0 - I_c$, which is estimated for small $I_{8\pi}$. Increasing further I_{ac}, we move into a regime where only even steps are observed. Finally, for higher values of I_{ac} we arrive to the situation where even and odd steps are present.

IV. ASYMPTOTIC LIMITS OF THE 2S-RSJ MODEL

We study two asymptotic limits of the 2S-RSJ model that have experimental relevance. First, the low-intensity limit $I_{ac} \ll I_c$ is the limit where we can expect to observe only even Shapiro steps even for $I_{4\pi}/I_{2\pi} \ll 1$. Second, the high-intensity limit $I_{ac} \gg I_c$, where both steps are present. Before entering into the study of the asymptotic limits, it is convenient to rewrite Eq. (1) using dimensionless units. We first divide Eq. (1) by the critical current I_c. Then, we make the change of variable

$$\tilde{t} = (2eRI_c/\hbar)t,$$

and substitute currents and frequencies as follows:

$$\tilde{I}_i = \frac{I_i}{I_c}, \quad \tilde{\omega}_{ac} = \frac{\hbar\omega_{ac}}{2eRI_c}.$$

Then, Eq. (1) yields

$$\tilde{I}_0 + \tilde{I}_{ac}\sin(\tilde{\omega}_{ac}\tilde{t}) = \frac{d\varphi}{d\tilde{t}} + \tilde{I}_{2\pi}\sin(\varphi) + \tilde{I}_{4\pi}\sin(\varphi/2). \quad (5)$$

In this notation, the critical current is normalized to 1, namely,

$$\tilde{I}_c = 1 = \max\{\tilde{I}_{2\pi}\sin(\varphi) + \tilde{I}_{4\pi}\sin(\varphi/2)\}. \quad (6)$$

Derived quantities such as the voltage or the frequency of the junction are given by $\tilde{\overline{V}} = \overline{V}/I_cR$ and $\tilde{\omega}_0 = \hbar\omega_0/2eRI_c$, respectively. Thus, the Josephson relation is $\tilde{V} = \tilde{\omega}_0$, showing that the voltage and the frequency of the junction are equal.

In order to keep the notation as simple as possible, from now on we skip the tildes, implying the dimensionless variables, and restore dimensionality in the conclusions. In these new units, we will study the low- ($I_{ac} \ll 1$) and the high-intensity limits ($I_{ac} \gg 1$).

A. Low-intensity limit: $I_{ac} \ll 1$

In this limit we treat the ac driving as a perturbation, thus, we expand $\varphi(t)$ in powers of I_{ac} [47,48], that is,

$$\varphi = \varphi_0 + I_{ac}\,\varphi_1 + I_{ac}^2\,\varphi_2 + \cdots.$$

The zeroth-order contribution φ_0 corresponds to the dc-driven solution of the 2S-RSJ equation and the φ_n is the nth-order correction. In this limit the width of the Shapiro steps is proportional to I_{ac}. In order to determine their width, we perform a trick [47,48] which consists of splitting I_0, which is a constant parameter, into

$$I_0 = I_v + I_{ac}\,\beta_1 + I_{ac}^2\,\beta_2 + \cdots.$$

Here, I_v is given by the value of I_0 at the beginning of the step. The rest of the terms (β_n) leave constant the voltage. In this way, the zeroth-order contribution determines the voltage $\langle\dot{\varphi}\rangle = \langle\dot{\varphi}_0\rangle$, yielding $\langle\dot{\varphi}_n\rangle = 0$, for $n \neq 0$. Therefore, we need to determine β_n that cancels the nth-order contribution of the voltage, i.e., $\langle\dot{\varphi}_n\rangle = 0$. As we will see below, this gives the step width: the range of I_0 in which the voltage remains constant.

1. *Zeroth-order contribution in I_{ac}: Power spectrum*

Using the above definitions, we obtain the zeroth-order differential equation

$$I_v = \dot{\varphi}_0 + I_{2\pi}\sin(\varphi_0) + I_{4\pi}\sin(\varphi_0/2). \quad (7)$$

Its exact analytical solution is cumbersome and does not provide any further insight with respect to the numerical solution. For this reason, we have adapted the solution of a 2π

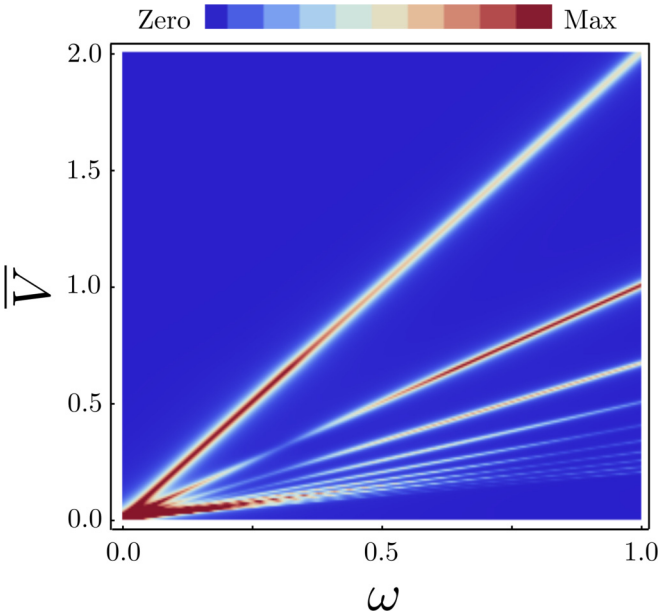

FIG. 6. Low-intensity limit $I_{\rm ac} \ll 1$: Fourier transform (color scale) $\dot{\varphi}_0(\omega) = |\int dt\, e^{i\omega t}\dot{\varphi}_0(t)|$ as a function of ω and the voltage $V = \omega_0$. The intensity of the resonances follow Eq. (9). The first two resonance lines with higher slope correspond to the frequencies $\omega = \omega_0/2$ (fractional frequency) and $\omega = \omega_0$. The rest of the resonance lines correspond to higher harmonics.

junction [47] taking into account the presence of two periods T_1 and T_2 given in Eqs. (3) and (4), and adjusting the intensity of the function. See further details in the Appendix. Doing so we obtain

$$\dot{\varphi}_0(t) \approx \omega_0\Bigg[1 + \sum_{n=1}^{\infty} z^n [2\cos(n\omega_0 T_1/4)\cos(n\omega_0 t/2) + (I_{2\pi} - 1)\sin(n\omega_0 T_1/4)\sin(n\omega_0 t/2)]\Bigg]. \quad (8)$$

Besides, the amplitudes of the harmonics decrease in geometric progression with $z = \sqrt{I_{\rm v} - \omega_0}$. This approximation shows the numerical solution coming out from Eq. (7) (see Appendix), especially for $I_{4\pi}/I_{2\pi} \leqslant 0.5$.

The Fourier transform of Eq. (8) is proportional to the emission spectrum of the voltage, and has been measured in Ref. [20]. Performing the Fourier transform of Eq. (8), $\dot{\varphi}_0(\omega) = |\int dt\, e^{i\omega t}\dot{\varphi}_0(t)|$ we obtain

$$\dot{\varphi}_0(\omega) \approx \delta(\omega - n\omega_0/2) z^n \omega_0 \Bigg[4\cos^2\left(\frac{nT_1}{T_1+T_2}\pi\right) + (I_{2\pi} - 1)^2 \sin^2\left(\frac{nT_1}{T_1+T_2}\pi\right)\Bigg]^{1/2}, \quad (9)$$

where the delta function $\delta(\omega - n\omega_0/2)$ makes $\dot{\varphi}_0(\omega)$ finite for $\omega = n\omega_0/2$, with $n = 1$ ($n = 2$) giving the fractional (integer) frequency $\omega_0/2$ (ω_0). Here, we have made use of the relation $\omega_0 = 4\pi/(T_1 + T_2)$.

In Fig. 6, we represent $\dot{\varphi}_0(\omega)$ as a function of ω and $V = \omega_0$. We will focus on the two top resonance lines, which correspond from top to bottom to the frequencies $\omega_0/2$ ($n = 1$, i.e., $\omega = \omega_0/2$) and ω_0 ($n = 2$, i.e., $\omega = \omega_0$), respectively. We can observe that the fractional contribution with $n = 1$ [$\dot{\varphi}_0(\omega_0/2)$] dominates over the 2π contribution with $n = 2$ [$\dot{\varphi}_0(\omega_0)$] for low values of ω_0. Increasing further ω_0, this tendency is reversed and the 2π contribution dominates. As we explained above, this can be understood in terms of the ratio T_1/T_2, which decreases as a function of I_0, as it was shown in Fig. 3(c) (note that ω_0 is tuned by I_0).

For simplicity, we analyze the limit where $I_{2\pi} \gg I_{4\pi}$, which yields in our dimensionless units $I_{2\pi} \sim 1$ making the second term in Eq. (9) negligible. In this scenario, the coefficient $\cos[n\pi T_1/(T_1 + T_2)]$ rules the periodicity of the voltage. In the limit where $T_1 \gg T_2$, $\cos^2[n\pi T_1/(T_1 + T_2)] \approx 1$, and the Fourier expansion contains only one frequency, i.e., $\omega_0/2$ and its harmonics. Therefore, the junction behaves like a pure 4π-periodic junction. In the opposite limit where $T_1 \sim T_2$, the arguments $T_1/(T_1 + T_2) \approx 1/2$, thus, Eq. (9) only contains even terms, and thus, the frequency $\omega_0/2$ is doubled to ω_0, yielding a 2π contribution. This $4\pi \to 2\pi$ transition is shown in Fig. 6 and is consistent with the emission spectrum experiment performed in Ref. [20]. The value of ω_0 at which the integer contribution $n = 2$ overcomes the fractional contribution $n = 1$ depends only on the ratio $I_{4\pi}/I_{2\pi}$. Thus, a direct comparison with the experimental results provides the value $I_{4\pi}$ [20].

2. *First-order contribution in $I_{\rm ac}$: Shapiro steps width*

The first-order contribution is obtained from the solution of the linear differential equation

$$\beta_1 + \sin(\omega_{\rm ac} t) = \dot{\varphi}_1 + \varphi_1\left(I_{2\pi}\cos(\varphi_0) + \frac{I_{4\pi}}{2}\cos(\varphi_0/2)\right), \quad (10)$$

which can be solved using the integrating factor $\exp\{\int dt[I_{2\pi}\cos(\varphi_0) + I_{4\pi}/2\cos(\varphi_0/2)]\}$. At this point it is particularly useful to realize that

$$I_{2\pi}\cos(\varphi_0) + \frac{I_{4\pi}}{2}\cos(\varphi_0/2) = -\frac{\ddot{\varphi}_0}{\dot{\varphi}_0}. \quad (11)$$

This relation simplifies greatly Eq. (10), yielding

$$\varphi_1(t) = \dot{\varphi}_0(t)\int_0^t dt'[\beta_1 + \sin(\omega_{\rm ac} t')]\frac{1}{\dot{\varphi}_0(t')}. \quad (12)$$

In order to extract the width of the first two Shapiro steps, we need to find the value of β_1 that makes $\langle\dot{\varphi}_1\rangle = 0$, that is, $\varphi_1(T)/T = 0$, where $T \to \infty$. This involves the cancellation of the constant terms in the integrand of Eq. (12). The rest of the terms are canceled by the factor $1/T$. Thus, when $\omega_{\rm ac} = n\omega_0/2$ we find the equality

$$\beta_1 f_0 + f_n \exp[i(\omega_{\rm ac} - n\omega_0/2)t] = 0, \quad (13)$$

where f_n are the Fourier coefficients of $1/\dot{\varphi}_0(t)$, namely,

$$\frac{1}{\dot{\varphi}_0(t)} = \sum_{n=-\infty}^{\infty} f_n \exp(in\omega_0 t/2). \quad (14)$$

The solution for $n = 1$ corresponds to the second step ($\omega_0 = 2\omega_{\rm ac}$), while for $n = 2$ to the first step ($\omega_0 = \omega_{\rm ac}$). The step width is given by the equation

$$\beta_1(n\omega_0/2) = 2\left|\frac{f_n}{f_0}\right|. \quad (15)$$

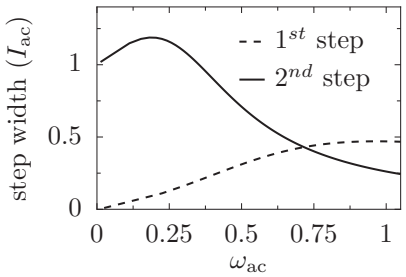

FIG. 7. Low-intensity limit $I_{ac} \ll 1$: first (dashed curve) and second (solid curve) Shapiro steps width in units of I_{ac} as a function of ω_{ac}. The width of the Shapiro steps is calculated from Eq. (15).

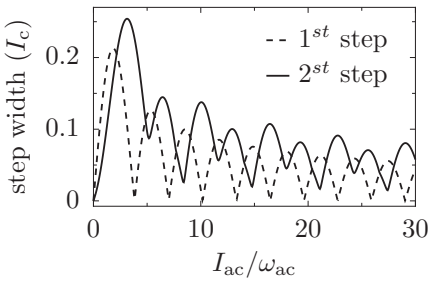

FIG. 8. High-intensity limit $I_{ac} \gg 1$: width of the first two steps as a function of I_{ac}/ω_{ac}. The oscillatory behavior is due to the Bessel functions [see Eqs. (21) and (22)]. Interestingly, even Shapiro steps exhibit a beating pattern produced by the coexistence of 2π and 4π supercurrents.

Note that in pure 2π junctions, the first-order contribution only contains solutions for the first step width. In turn, when both contributions are present, the first-order contribution provides the width of the first and the second steps. In Fig. 7 we show the value of $\beta_1(n\omega_0/2)$ (the step width) as a function of ω_{ac}. We can observe that the second step dominates for low values of ω_{ac}, and decreases at higher values. This behavior is rather similar to the one observed in the power spectrum, where for $I_0 - I_c \lesssim \sqrt{2}I_{4\pi}$, the fractional signal is more visible. Therefore, we can establish the connection between the periodicity of the Shapiro experiment and the radiated power spectrum observed in Refs. [17–20] since we see from Eq. (15) that the Shapiro steps are proportional to the Fourier transform of $1/\dot{\varphi}_0(t)$.

Higher Shapiro steps can be calculated by taking further higher orders in φ_n and β_n [48]. The resulting differential equations are still linear, however, their solution becomes cumbersome. Hence, it is difficult to gain further analytical understanding of the higher Shapiro steps.

B. High-intensity limit: $I_{ac} \gg 1$

In this limit, the zeroth-order contribution is obtained neglecting the supercurrent contributions, thus,

$$I_0 + I_{ac}\sin(\omega_{ac}t) = \frac{d\varphi_0(t)}{dt}, \tag{16}$$

where $\varphi_0(t)$ is the zeroth contribution, in units of I_c. Equation (16) can be integrated exactly,

$$\varphi_0(t) = I_0 t - \frac{I_{ac}}{\omega_{ac}}\cos(\omega_{ac}t) + \phi_0, \tag{17}$$

where ϕ_0 is a constant phase that needs to be determined (see below). Since we have linearized the differential equation, the average voltage at zeroth order is $\langle\dot{\varphi}_0\rangle = I_0$. In order to recover the Shapiro steps we need to take into account the first-order contribution, given by

$$\frac{d\varphi_1(t)}{dt} = -I_{2\pi}\sin[\varphi_0(t)] - I_{4\pi}\sin[\varphi_0(t)/2]. \tag{18}$$

$\dot{\varphi}_1(t)$ can be explicitly written by plugging Eq. (17) into Eq. (18), and taking the Jacobi-Anger expansion

$$\dot{\varphi}_1(t) = -\frac{1}{2}\sum_{n=-\infty}^{\infty}\left[I_{2\pi}J_n\left(\frac{I_{ac}}{\omega_{ac}}\right)\sin[(\omega_0 - n\omega_{ac})t + \phi_0] + I_{4\pi}J_n\left(\frac{I_{ac}}{2\omega_{ac}}\right)\sin[(\omega_0/2 - n\omega_{ac})t + \phi_0/2]\right], \tag{19}$$

where $J_n(x)$ is the nth Bessel function. The time average of Eq. (19) is finite for $\omega_0 = n\omega_{ac}$, namely,

$$\langle\dot{\varphi}_1\rangle = -\frac{1}{2}\left[I_{2\pi}J_n\left(\frac{I_{ac}}{\omega_{ac}}\right)\sin(\phi_0)\delta(\omega_0 - n\omega_{ac}) + I_{4\pi}J_n\left(\frac{I_{ac}}{2\omega_{ac}}\right)\sin(\phi_0/2)\delta(\omega_0/2 - n\omega_{ac})\right]. \tag{20}$$

Shapiro steps arise choosing the value of ϕ_0 that compensates the increment of I_0, and thus $\langle\dot{\varphi}_0\rangle + \langle\dot{\varphi}_1\rangle = n\omega_{ac}$ for different values of I_0. Therefore, the step widths will be given by the extreme value of Eq. (19) in respect to ϕ_0 for the interval $\phi_0 = [0,4\pi]$. Under these approximations, odd and even Shapiro steps are given by

$$\Delta_{2n-1} = \frac{1}{2}I_{2\pi}\left|J_{2n-1}\left(\frac{I_{ac}}{\omega_{ac}}\right)\right|, \tag{21}$$

$$\Delta_{2n} = \frac{1}{2}\mathrm{Max}\left\{I_{2\pi}J_{2n}\left(\frac{I_{ac}}{\omega_{ac}}\right)\sin(\phi_0) + I_{4\pi}J_n\left(\frac{I_{ac}}{2\omega_{ac}}\right)\sin(\phi_0/2)\right\}, \tag{22}$$

where Δ_n is the nth step width given in units of I_c. In Fig. 8, we represent Δ_n for $n = 1$ and 2 as a function of I_{ac}/ω_{ac}. It is important to note that both terms $I_{2\pi}$ and $I_{4\pi}$ enter in the same way in the step widths. Therefore, even steps can only dominate for $I_{4\pi}/I_{2\pi} \gg 1$. Furthermore, we observe in Fig. 8 a genuine oscillatory pattern. Odd step widths show a typical oscillatory pattern, i.e., they involve only one Bessel function and, thus, they go to zero for given values of the argument I_{ac}/ω_{ac}. In turn, the even step widths are composed by the sum of two different Bessel functions. Thus, the step widths show two minima, and none of them reaches zero. Therefore, although the even step widths are comparable with the odd step widths, the beating pattern of the step widths can be used to identify and estimate the intensity of the 4π component of the supercurrent.

V. CONCLUSIONS

In this paper, we study the dynamics of a Josephson junction carrying two superconducting contributions: a 2π and a 4π periodic in phase difference, with intensity $I_{2\pi}$ and $I_{4\pi}$, respectively. We use the 2S-RSJ model to understand the

relation between the dynamics of the junction and the width of the Shapiro steps, and in particular we focus on the reasons that make the even steps dominate over the odd steps for a fixed ratio $I_{4\pi}/I_{2\pi} \ll 1$. This phenomenon [31] is important because it has been observed in different experiments [17,18,20], and could help to determine the presence of topological superconductivity.

We provide a qualitative explanation of this phenomenon in terms of the washboard potential, and obtain a phase diagram of the widths of the Shapiro steps as a function of I_{ac} and I_0. Remarkably, using some elementary reasonings we find the range of ac bias, i.e., I_{ac}, where the nonlinear dynamics of the junction causes a regime in which the even steps dominate over the odd steps. Increasing further I_{ac} we expect to find a crossover to a situation where odd steps are present although even steps dominate. Then, at very high values of I_{ac}, both contributions become comparable.

Furthermore, we study analytically the Shapiro step width as a function of ω_{ac} in two different limits of I_{ac}: the low-intensity limit $I_{ac} \ll I_c$ and the high-intensity limit $I_{ac} \gg I_c$. The low-intensity limit is precisely the limit where one can find only even Shapiro steps even when $I_{4\pi}/I_{2\pi} \ll 1$. In this limit, we find the link between two different experiments: the Josephson emission spectrum [20] and the Shapiro experiment [17–19]. In addition, we obtain analytical expressions for the step widths in the high-intensity limit $I_{ac} \gg I_c$. We show that the maximum width of the even and odd Shapiro steps depends linearly on the ratio of $I_{4\pi}/I_{2\pi}$. However, even in this regime one can unravel the existence of the 4π-periodic contribution, due to the beating pattern of even Shapiro steps as a function of I_{ac}.

ACKNOWLEDGMENTS

We acknowledge financial support from the DFG via Grant No. SFB 1170 "ToCoTronics," the Land of Bavaria (Institute for Topological Insulators and the Elitenetzwerk Bayern), the German Research Foundation DFG (Grant No. SPP 1666), the European Research Council (advanced grant project 3-TOP), the Helmholtz Association (VITI) and the Spain's MINECO through Grant No. MAT2014-58241-P. T.M.K. is financially supported by the European Research Council Advanced Grant No. 339306 (METIQUM) and by the Ministry of Education and Science of the Russian Federation under Contract No. 14.B25.31.007. T.M.K., E.B., and L.W.M. gratefully thank the Alexander von Humboldt foundation for a Research-prize. R.S.D. acknowledges support from Grants-in-Aid for Young Scientists B (Grant No. 26790008) and Grants-in-Aid for Scientific Research A (Grant No. 16H02204). We acknowledge enlightening discussions with Y. V. Nazarov, J. Picó, C. Brüne, and H. Buhmann.

APPENDIX: ADAPTING THE 2π SOLUTION TO THE MIXED SITUATION

The solution of Eq. (5) with $I_{4\pi} = 0$ and $I_{2\pi} = 1$ has been solved previously in Ref. [47]:

$$T = \int_0^{2\pi} \frac{d\varphi}{I_v - \sin(\varphi)} = \frac{2\pi}{\sqrt{I_v^2 - 1}}. \tag{A1}$$

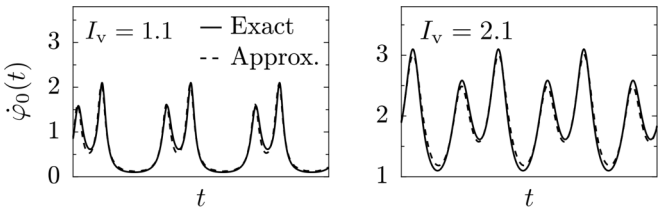

FIG. 9. Comparison between the numerical solution of Eq. (5) $\dot{\varphi}_0(\tau)$ (solid lines) and the approximate solution given by Eq. (8) (dashed lines). We have used $I_{4\pi}/I_{2\pi} = 0.5$. We compare two different values of $I_v = 1.1$ (left panel) and $I_v = 2.1$ (right panel).

The corresponding frequency $\omega_0 = 2\pi/T$ is proportional to the voltage. Besides, the stationary voltage is equal to the frequency $V = \omega_0 = \sqrt{I_v^2 - 1}$. In this case, the time evolution of $\dot{\varphi}_0(t)$ can be solved exactly and is given by

$$\dot{\varphi}_0(t) = \omega_0 \left[1 + 2 \sum_{n=1}^{\infty} (I_v - \omega_0)^n \cos(n\omega_0 t) \right] \tag{A2}$$

for $I_v > 1$. In order to adapt this solution to the more general case, where $I_{4\pi} \neq 0$, we need to take into account the two periods T_1 and T_2, and also to include the different intensities observed in the maxima F_1, F_2, S_1, and S_2 [see Fig. 3(a)]. To this aim, we double the period of the system by substituting ω_0 by $\omega_0/2$, with $\omega_0 = 4\pi/T_{4\pi}$, and then shift the cosine term in two opposite directions $\pm T_1/2$. In this way, we tune from a solution that exhibits equally time spaced peaks, where the period T is given by Eq. (A1), to a function exhibiting peaks separated by T_1 and T_2. In order to include two periods T_1 and T_2 maintaining the same height one needs to renormalize the Fourier coefficients and substitute $(I_v - \omega_0)$ by its square root of $z = (I_v - \omega_0)^{1/2}$, yielding

$$\dot{\varphi}_0(t) \approx \omega_0 \left[1 + \sum_{n=1}^{\infty} z^n \{ \cos[n\omega_0 (t + T_1/2)/2] + \sin[n\omega_0 (t - T_1/2)/2] \} \right]. \tag{A3}$$

This equation gives rise to peaks exhibiting equal height, in order to adjust to the numerical solution, we multiply the second term in the sum by $I_{2\pi}$, which in the pure 2π solution was equal to 1, namely,

$$\dot{\varphi}_0(t) \approx \omega_0 \left[1 + \sum_{n=1}^{\infty} z^n [(I_{2\pi} + 1) \cos(n\omega_0 T_1/4) \cos(n\omega_0 t/2) + (I_{2\pi} - 1) \sin(n\omega_0 T_1/4) \sin(n\omega_0 t/2)] \right]. \tag{A4}$$

We find that the equation becomes more similar to the numerical results when we substitute the first coefficient by 2, that is, $(I_{2\pi} + 1) \to 2$, yielding the result given in Eq. (8). In Fig. 9 we show how accurate the approximate solution is, by comparing it against the numerical result.

[1] N. Read and D. Green, Phys. Rev. B **61**, 10267 (2000).
[2] D. A. Ivanov, Phys. Rev. Lett. **86**, 268 (2001).
[3] X.-L. Qi and S.-C. Zhang, Rev. Mod. Phys. **83**, 1057 (2011).
[4] A. Nayak, S. H. Simon, A. Stern, M. Friedman, and S. D. Sarma, Rev. Mod. Phys. **80**, 1083 (2008).
[5] J. Alicea, Y. Oreg, G. Refael, F. von Oppen, and M. P. A. Fisher, Nat. Phys. **7**, 412 (2011).
[6] J. Alicea, Rep. Prog. Phys. **75**, 076501 (2012).
[7] A. Stern and N. H. Lindner, Science **339**, 1179 (2013).
[8] A. P. Mackenzie and Y. Maeno, Rev. Mod. Phys. **75**, 657 (2003).
[9] L. Elster, C. Platt, R. Thomale, W. Hanke, and E. M. Hankiewicz, Nat. Commun. **6**, 8232 (2015).
[10] A. Y. Kitaev, Phys. Usp. **44**, 131 (2001).
[11] L. Fu and C. L. Kane, Phys. Rev. B **79**, 161408(R) (2009).
[12] R. M. Lutchyn, J. D. Sau, and S. Das Sarma, Phys. Rev. Lett. **105**, 077001 (2010).
[13] Y. Oreg, G. Refael, and F. von Oppen, Phys. Rev. Lett. **105**, 177002 (2010).
[14] V. Mourik, K. Zuo, S. M. Frolov, S. R. Plissard, E. P. A. M. Bakkers, and L. P. Kouwenhoven, Science **336**, 1003 (2012).
[15] A. Das, Y. Ronen, Y. Most, Y. Oreg, M. Heiblum, and H. Shtrikman, Nat. Phys. **8**, 887 (2012).
[16] S. M. Albrecht, A. P. Higginbotham, M. Madsen, F. Kuemmeth, T. S. Jespersen, J. Nygård, P. Krogstrup, and C. M. Marcus, Nature (London) **531**, 206 (2016).
[17] L. P. Rokhinson, X. Liu, and J. K. Furdyna, Nat. Phys. **8**, 795 (2012).
[18] J. Wiedenmann, E. Bocquillon, R. S. Deacon, S. Hartinger, O. Herrmann, T. M. Klapwijk, L. Maier, C. Ames, C. Brüne, C. Gould, A. Oiwa, K. Ishibashi, S. Tarucha, H. Buhmann, and L. W. Molenkamp, Nat. Commun. **7**, 10303 (2016).
[19] E. Bocquillon, R. S. Deacon, J. Wiedenmann, P. Leubner, T. M. Klapwijk, C. Brüne, K. Ishibashi, H. Buhmann, and L. W. Molenkamp, Nat. Nanotechnol. **12**, 137 (2017).
[20] R. S. Deacon, J. Wiedenmann, E. Bocquillon, F. Domínguez, T. M. Klapwijk, P. Leubner, C. Brüne, E. M. Hankiewicz, S. Tarucha, K. Ishibashi, H. Buhmann, and L. W. Molenkamp, Phys. Rev. X **7**, 021011 (2017).
[21] H. J. Kwon, K. Sengupta, and V. M. Yakovenko, Eur. Phys. J. B **37**, 349 (2004).
[22] C. W. J. Beenakker, J. M. Edge, J. P. Dahlhaus, D. I. Pikulin, S. Mi, and M. Wimmer, Phys. Rev. Lett. **111**, 037001 (2013).
[23] F. Crépin and B. Trauzettel, Phys. Rev. Lett. **112**, 077002 (2014).
[24] S. Shapiro, Phys. Rev. Lett. **11**, 80 (1963).
[25] J. C. Budich, S. Walter, and B. Trauzettel, Phys. Rev. B **85**, 121405 (2012).
[26] D. Rainis and D. Loss, Phys. Rev. B **85**, 174533 (2012).
[27] B. van Heck, F. Hassler, A. R. Akhmerov, and C. W. J. Beenakker, Phys. Rev. B **84**, 180502(R) (2011).
[28] D. M. Badiane, M. Houzet, and J. S. Meyer, Phys. Rev. Lett. **107**, 177002 (2011).
[29] P. San-Jose, E. Prada, and R. Aguado, Phys. Rev. Lett. **108**, 257001 (2012).
[30] D. I. Pikulin and Y. V. Nazarov, Phys. Rev. B **86**, 140504(R) (2012).
[31] F. Domínguez, F. Hassler, and G. Platero, Phys. Rev. B **86**, 140503(R) (2012).
[32] M. Houzet, J. S. Meyer, D. M. Badiane, and L. I. Glazman, Phys. Rev. Lett. **111**, 046401 (2013).
[33] P. Virtanen and P. Recher, Phys. Rev. B **88**, 144507 (2013).
[34] P. San-Jose, J. Cayao, E. Prada, and R. Aguado, New J. Phys. **15**, 075019 (2013).
[35] P. Matthews, P. Ribeiro, and A. M. García-García, Phys. Rev. Lett. **112**, 247001 (2014).
[36] J. D. Sau and F. Setiawan, Phys. Rev. B **95**, 060501 (2017).
[37] G. Tkachov and E. M. Hankiewicz, Phys. Rev. B **88**, 075401 (2013).
[38] I. Sochnikov, L. Maier, C. A. Watson, J. R. Kirtley, C. Gould, G. Tkachov, E. M. Hankiewicz, C. Brüne, H. Buhmann, L. W. Molenkamp, and K. A. Moler, Phys. Rev. Lett. **114**, 066801 (2015).
[39] B. Sothmann and E. M. Hankiewicz, Phys. Rev. B **94**, 081407 (2016).
[40] F. Zhang and C. L. Kane, Phys. Rev. Lett. **113**, 036401 (2014).
[41] C. P. Orth, R. P. Tiwari, T. Meng, and T. L. Schmidt, Phys. Rev. B **91**, 081406 (2015).
[42] Y. Peng, Y. Vinkler-Aviv, P. W. Brouwer, L. I. Glazman, and F. von Oppen, Phys. Rev. Lett. **117**, 267001 (2016).
[43] Yu. M. Ivanchenko, Zh. Eksp. Teor. Fiz. **51**, 337 (1966) [Sov. Phys. JETP **24**, 225 (1967)].
[44] W. C. Stewart, Appl. Phys. Lett. **12**, 277 (1968).
[45] D. E. McCumber, J. Appl. Phys. **39**, 3113 (1968).
[46] S. M. Albrecht, E. B.Hansen, A. P. Higginbotham, F. Kuemmeth, T. S. Jespersen, J. Nygård, P. Krogstrup, J. Danon, K. Flensberg, and C. M. Marcus, Phys. Rev. Lett. **118**, 137701 (2017).
[47] L. G. Aslamazov, A. I. Larkin, and Yu. N. Ovchinnikov, Zh. Eksp. Teor. Fiz. **9**, 150 (1969) [Sov. Phys. JETP **9**, 87 (1969)].
[48] E. D. Thompson, J. Appl. Phys. **44**, 5587 (1973).